

activity of fibroblast growth factors (11). Based on these findings, we have demonstrated in our previous work using X-ray photoelectron spectroscopy that polyphosphoric acid (PPA) can be tightly adsorbed to the Ti surface in a dose-dependent manner (12). In addition, we reported that a Ti surface treated with PPA significantly enhanced initial attachment and proliferation of two types of cells, namely, human bone marrow-derived mesenchymal stem cells and mouse osteoblast-like cells (12, 13). We could demonstrate that these accelerated cell responses were not due to increased surface roughness induced by PPA, but rather must be ascribed to the biological effect of PPA itself (12). In this way, treatment of Ti with PPA might be a new methodology to fabricate bioactive Ti implants.

In order to assess the potential promoting effect of this Ti surface modification on bone regeneration around implants, we have now carried out an *in vivo* study using a rat model. The study was conducted to compare the bone-implant contact ratio (BICR) of Ti implants treated with three different concentrations (0, 1 and 10 wt%) of PPA. The null hypothesis tested in this study was that there is no difference in BICR amongst Ti implants treated with the three differently concentrated PPA solutions.

Materials and methods

Animal

Eight-week-old-male Wister rats ($n = 30$) were housed in a temperature-controlled room with a 12-h alternating light-dark cycle and were given water and food *ad lib* throughout the study. The Animal Care Use Review Committee of the Okayama University Dental School approved the experimental protocol in this study (OK-2006314).

Titanium implant surface treatment

Commercially available pure Ti cylinders* (Grade-II; 2 mm in diameter, 4 mm in length) were used in this study. As shown in Fig. 1, part of the cylinder was narrowed to a diameter of 1 mm. The Ti cylinders were first cleaned by ultrasonic rinsing successively in trichloroethylene and ethanol (10 min each). They were then immersed in two different solutions of PPA[†]

*GC, Tokyo, Japan.

[†]WAKO, Osaka, Japan.

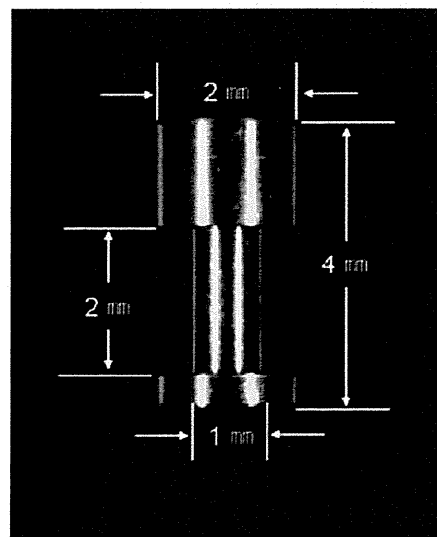


Fig. 1. The titanium implant utilized in this study.

with concentrations of 1 and 10 wt% for 24 h at 37 °C. Ti cylinders cleaned and immersed in distilled water for 24 h at 37 °C served as control. After each surface treatment, each cylinder was washed three times with distilled water (PPA is very soluble in water and any unreacted acid is therefore easily removed) and autoclaved.

Implantation

The animals were anaesthetized using ketamine hydrochloride (35 mg kg⁻¹) and xylazine hydrochloride (12 mg kg⁻¹). Both the tibiae were shaved and disinfected, and a full thickness incision was made on the dorsal aspect of the tibiae. Implant sites were drilled under cooled sterile saline irrigation using a twist drill[‡] (diameter of 2.0 mm). The three differently treated Ti cylinders were randomly implanted into the prepared holes in the tibiae ($n = 20$ per experimental group). The wound was then sutured. The rats were allowed to recover and were housed as described above.

Section preparation

Two or four weeks after operation, the animals were deeply anaesthetized with diethyl ether and perfused through the abdominal aorta with physiological saline,

[‡]Nobel Biocare AB, Gotenberg, Sweden.

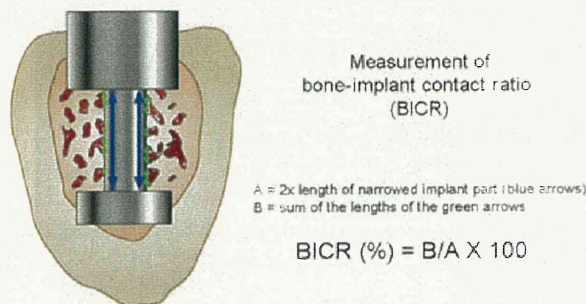


Fig. 2. Schematic drawing explaining the measurement of the bone-implant contact ratio (BICR).

followed by a fixative containing 10% paraformaldehyde and 5% glutaraldehyde in 0.1 M phosphate buffer. After the tibiae were dissected ($n = 30$ tibiae for each time interval, of which 10 per experimental group), the samples containing the implants were trimmed and immersed in the same fixative for 1 week. The specimens were dehydrated in graded ethanol and styrene, and then embedded in polyester resin, (Rigolac).[§] The embedded materials were polymerized, after which undecalcified sections were ground parallel to the long axis of the implant to a thickness of approximately 70 μm using an ECOMET3 grinding system.[¶]

Histological and histometrical analysis

The sections were double-stained with basic fuchsin and methylene blue, and then imaged by light microscopy (BioZero BZ-8000).^{**} Using the photomicrographs of each section, the BICR of the implant was determined semi-automatically by three examiners blinded to the experimental group using the commercially available BZ Analyzer software^{**} (Fig. 2). As shown in Fig. 2, the BICR was evaluated only in the narrow portion of the implant. Mean BICR data determined by three examiners were calculated in each section and submitted for statistical analysis. The statistical analysis was performed using one-way ANOVA followed by Scheffe's multiple comparison tests.

[§]Nissin EM, Tokyo, Japan.

[¶]Buehler, Lake Bluff, IL, USA.

^{**}KEYENCE, Osaka, Japan.

Results

Histological findings

Histological observation of the sections that were prepared 2 weeks after implantation revealed that new bone formation was observed in direct contact with the Ti surface in all the experimental conditions. Additionally, bone trabeculae with a mesh-like structure were seen in the medullary canal (Fig. 3, arrows). Those bone trabeculae in the PPA-treated Ti implants were somewhat denser than those in the control untreated Ti implants. However, those mesh-like structures tended to disappear 4 weeks after implantation in all the experimental conditions (Fig. 4). With regard to the newly formed bone trabeculae at the interface between Ti and medulla, those in the PPA-treated groups seemed abundant, both 2 and 4 weeks after implantation. Especially, 4 weeks after implantation, consecutive bone trabeculae formation was observed in the PPA-treated Ti implant groups (Fig. 4).

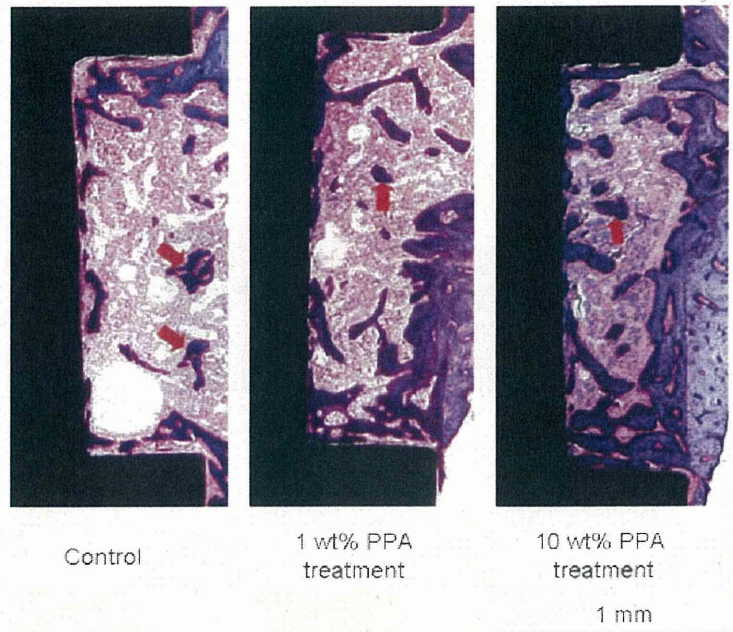
Histometrical findings

Regarding BICR analysis, statistics revealed that PPA treatment of the Ti implant surface significantly enhanced direct bone contact to the Ti surface. Especially the BICRs of the 1 wt% PPA-treated Ti implants were significantly higher than those of the control untreated Ti implants, both 2 and 4 weeks after implantation (Fig. 5). At the latter observation period, the mean BICR of the 10 wt% PPA treatment implants was also significantly higher than that of the untreated Ti implants.

Discussion

In this study, we utilized Ti cylinders with the major middle part narrowed. We then quantified the amount of bone formation along the vertical axis of the implant, but only at the narrowed area. When such a Ti cylinder was implanted into the prepared hole in the tibia, the area around the narrowed implant part got filled with a blood clot so that there was no direct contact with cancellous bone. As cancellous bone involves abundant bone-related cells (e.g. osteoblasts, mesenchymal stem cells), we prevented in this way that such bone-related cells would directly attach to and proliferate on the adjacent Ti surface (osseointegration). Therefore, this

Fig. 3. Representative histological images of sections through the bone-implant interface 2 week after implantation. Bone trabeculae with mesh-like structures (arrows) were seen in the medullary canal in all experimental conditions. The newly formed bone trabeculae in contact with the Ti surface tended to be thicker when the Ti surface was treated with polyphosphoric acid (PPA).

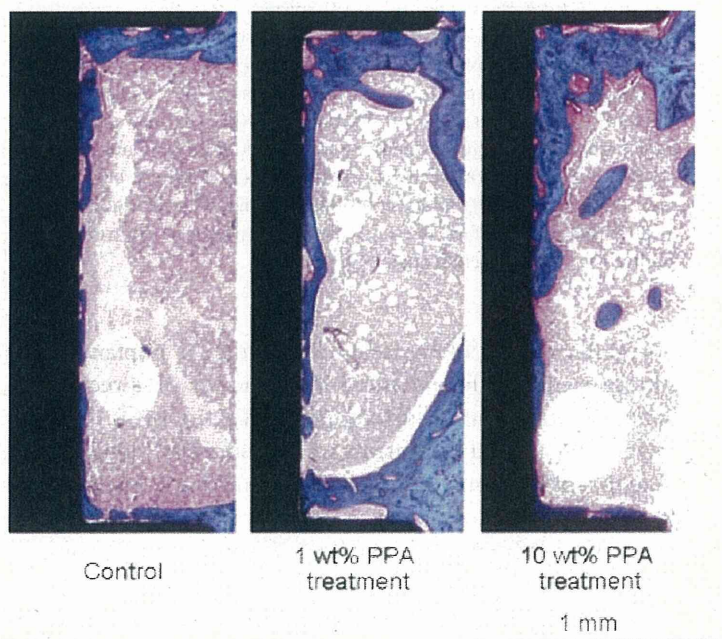


model allowed us to evaluate the effect of PPA treatment of the Ti surface on bone regeneration around the implant.

Two weeks after implantation, new bone formation in direct contact with the Ti surface was observed in all the experimental conditions. Furthermore, bone with a mesh-like structure was clearly present in the medullary canal. These trabeculae most likely result

from the inflammatory response to the implantation. The bone trabeculae around the PPA-treated Ti implants were somewhat thicker than those around the control untreated Ti implants. Four weeks after implantation, most mesh-like bone structures disappeared in all the experimental conditions. These findings are consistent with other previous reports (14, 15).

Fig. 4. Representative histological images of sections through the bone-implant interface 4 week after implantation. The bone trabeculae with mesh-like structures that were observed in the medullary canal 2 weeks after implantation, disappeared at this stage. Two weeks after implantation, the newly formed bone trabeculae in contact with the Ti surface tended to be thicker when the Ti surface was treated with polyphosphoric acid (PPA).



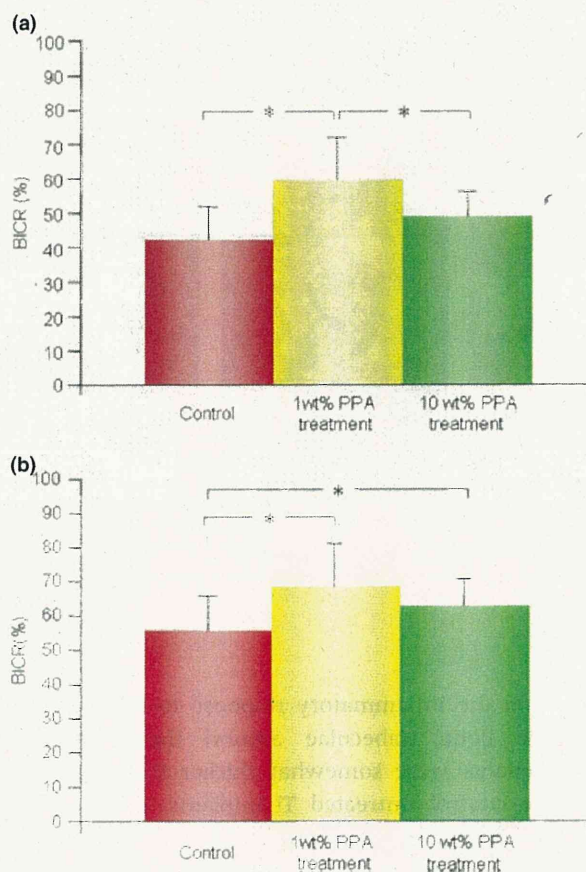


Fig. 5. The mean bone-implant contact ratio (BICR) of the untreated and treated Ti implants 2 and 4 weeks after implantation ($n = 10$ for each condition). (a) The mean BICR 2 weeks after implantation. The mean BICR of the 1 wt% polyphosphoric acid (PPA)-treated Ti implants was significantly higher than that of the untreated control and the 10 wt% PPA-treated Ti implants 2 weeks after implantation. (b) The mean BICR 4 weeks after implantation. Although 4 weeks after implantation, the mean BICR of the 1 wt% PPA-treated Ti implants was the highest, both the 1 and 10 wt% PPA treatment resulted in a significantly higher mean BICR than that of the untreated Ti implants in control. *Indicates statistical significance ($P < 0.05$).

Regarding BICR, PPA treatment of the Ti implant surface significantly enhanced the amount of direct bone contact to the Ti surface. Especially, the BICR of 1 wt% PPA-treated Ti implants was significantly higher than that of the control Ti implants, both 2 and 4 weeks after implantation. At 4 weeks, 10 wt% PPA treatment also significantly increased the BICR as compared to the BICR of the control Ti implants. Such early and abundant bone formation surrounding an implant must contribute to the implant stability. Hence, surface

treatment of Ti implants with PPA was shown to be an effective method to modify the Ti surface for improved osseointegration.

This enhanced bone formation around PPA-treated Ti implants must most likely be ascribed to an accelerated cell response to PPA that was adsorbed on the Ti implant surface, as we demonstrated before using X-ray photoelectron spectroscopy (12). Our previous *in vitro* research also revealed that PPA bound to the Ti surface induced several biological effects on cultured cells (12, 13). More specifically, proliferation of human mesenchymal stem cells as well as mouse osteoblast-like cells was found to have extremely accelerated PPA-treated Ti surfaces in a dose-dependent manner. Nevertheless, some contradiction exists between the results of our previous *in vitro* cell culture data and our current *in vivo* BICR data. While a higher concentration of PPA resulted in a more accelerated cell proliferation, the BICR data in this study indicated that the 1 wt% PPA treatment was superior to the highly concentrated (10 wt%) PPA treatment. On the other hand, the newly formed bone trabeculae that contacted the Ti surface tended to be thicker when the cylinders were treated with PPA and this phenomenon seemed most obvious for the 10 wt% PPA treatment. Like BICR, the thickness of the bone trabeculae may also contribute to the implant stabilization in order to distribute masticatory and other oral stress. Therefore, also measurement of the bone trabeculae thickness might be a useful index to assess the effect of Ti surface treatments on bone regeneration in search for clinically useful bioactive implants.

In summary, the present *in vivo* data that PPA treatment of the Ti surface lead to more abundant bone formation in contact with the implant suggests that this method may shorten the healing period after implant placement. From a clinical point of view, this PPA surface treatment may be advantageous as compared to methods that coat the Ti surface with various bioactive substances. As most of these bioactive substances are proteins, careful attention is needed not to lose their biological activity before implant placement. In this way, Ti implant surface modification using PPA is simple and does not need special handling afterwards. For further development of this PPA treatment of Ti implants towards clinical application, more studies are definitely needed to determine the most optimal PPA treatment conditions that induce the rapidest and most abundant bone

formation around the implant, especially using animals that are closely related to human beings (e.g. beagle dogs, monkeys).

Acknowledgments

This study was supported in part by a Grant-in-Aid for Scientific Research from the Ministry of Education, Science, Sports and Culture of Japan (#17390516).

References

- Cooper LF. A role for surface topography in creating and maintaining bone at titanium endosseous implants. *J Prosthet Dent.* 2000;84:522–534.
- Rupp F, Scheideler L, Rehbein D, Axmann D, Geis-Gerstorfer J. Roughness induced dynamic changes of wettability of acid etched titanium implant modifications. *Biomaterials.* 2004;25:1429–1438.
- Rupp F, Scheideler L, Olshanska N, De Wild M, Wieland M, Geis-Gerstorfer J. Enhancing surface free energy and hydrophilicity through chemical modification of microstructured titanium implant surfaces. *J Biomed Mater Res A.* 2006;76:323–334.
- Kim MJ, Kim CW, Lim YJ, Heo SJ. Microrough titanium surface affects biologic response in MG63 osteoblast-like cells. *J Biomed Mater Res A.* 2006;79:1023–1032.
- Shalabi MM, Gortemaker A, Van't Hof MA, Jansen JA, Creugers NH. Implant surface roughness and bone healing: a systematic review. *J Dent Res.* 2006;85:496–500.
- Sul YT, Johansson C, Albrektsson T. Which surface properties enhance bone response to implants? Comparison of oxidized magnesium, TiUnite, and Osseotite implant surfaces *Int J Prosthodont.* 2006;19:319–328.
- Hayakawa T, Yoshinari M, Nemoto K. Direct attachment of fibronectin to tressyl chloride-activated titanium. *J Biomed Mater Res A.* 2003;67:684–688.
- Park JM, Koak JY, Jang JH, Han CH, Kim SK, Heo SJ. Osseointegration of anodized titanium implants coated with fibroblast growth factor-fibronectin (FGF-FN) fusion protein. *Int J Oral Maxillofac Implants.* 2006;21:859–866.
- Hilbig H, Kirsten M, Rupietta R, Graf HL, Thalhammer S, Strasser S *et al.* Implant surface coatings with bone sialoprotein, collagen, and fibronectin and their effects on cells derived from human maxillar bone. *Eur J Med Res.* 2007;12:6–12.
- Liu Y, Enggist L, Kuffer AF, Buser D, Hunziker EB. The influence of BMP-2 and its mode of delivery on the osteoconductivity of implant surfaces during the early phase of osseointegration. *Biomaterials.* 2007;28:2677–2686.
- Shiba T, Nishimura D, Kawazoe Y, Onodera Y, Tsutsumi K, Nakamura R *et al.* Modulation of mitogenic activity of fibroblast growth factors by inorganic polyphosphate. *J Biol Chem.* 2003;278:26788–26792.
- Maekawa K, Yoshida Y, Mine A, Fujisawa T, Van Meerbeek B, Suzuki K *et al.* Chemical interaction of polyphosphoric acid with titanium and its effect on human bone marrow derived mesenchymal stem cell behavior. *J Biomed Mater Res A.* 2007;82:195–200.
- Maekawa K, Yoshida Y, Mine A, Van Meerbeek B, Suzuki K, Kuboki T. Effect of polyphosphoric-acid pre-treatment of titanium on attachment, proliferation and differentiation of osteoblast like cells (MC3T3-E1). *Clin Oral Implants Res.* 2008;19:320–325.
- Takeshita F, Morimoto K, Suetsugu T. Tissue reaction to alumina implants inserted into the tibiae of rats. *J Biomed Mater Res.* 1993;27:421–428.
- Ayukawa Y, Okamura A, Koyano K. Simvastatin promotes osteogenesis around titanium implants. *Clin Oral Implants Res.* 2004;15:346–350.

Correspondence: Takuo Kuboki DDS, PhD, Professor and Chair, Department of Oral Rehabilitation and Regenerative Medicine, Okayama University Graduate School of Medicine and Dentistry and Pharmaceutical Sciences, 2-5-1 Shikata-cho, Okayama 700-8525, Japan.
E-mail: kuboki@md.okayama-u.ac.jp

CCN Family 2/Connective Tissue Growth Factor Modulates BMP Signalling as a Signal Conductor, Which Action Regulates the Proliferation and Differentiation of Chondrocytes

Azusa Maeda^{1,2}, Takashi Nishida¹, Eriko Aoyama³, Satoshi Kubota¹, Karen M. Lyons⁴, Takuo Kuboki² and Masaharu Takigawa^{1,*}

¹Department of Biochemistry and Molecular Dentistry; ²Department of Oral Rehabilitation and Regenerative Medicine, Okayama University Graduate School of Medicine, Dentistry and Pharmaceutical Sciences, Okayama, Japan; ³Biodental Research Center, Okayama University Dental School, Okayama, Japan; and ⁴Department of Orthopaedic Surgery, David Geffen School of Medicine at UCLA, CA, USA

Received September 9, 2008; accepted November 17, 2008; published online November 27, 2008

Both CCN family 2/connective tissue growth factor (CCN2/CTGF) and bone morphogenetic protein (BMP)-2 play an important role in cartilage metabolism. We evaluated whether or not CCN2 would interact with BMP-2, and examined the combination effect of CCN2 with BMP-2 (CCN2-BMP-2) on the proliferation and differentiation of chondrocytes. Immunoprecipitation-western blotting analysis, solid-phase binding assay and surface plasmon resonance (SPR) spectroscopy showed that CCN2 directly interacted with BMP-2 with a dissociation constant of 0.77 nM as evaluated by SPR. An *in vivo* study revealed that CCN2 was co-localized with BMP-2 at the pre-hypertrophic region in the E18.5 mouse growth plate. Interestingly, CCN2-BMP-2 did not affect the BMP-2/CCN2-induced phosphorylation of p38 MAPK but caused less phosphorylation of ERK1/2 in cultured chondrocytes. Consistent with these results, cell proliferation assay showed that CCN2-BMP-2 stimulated cell growth to a lesser degree than by either CCN2 or BMP-2 alone, whereas the expression of chondrocyte marker genes and proteoglycan synthesis, representing the mature chondrocytic phenotype, was increased collaboratively by CCN2-BMP-2 treatment in cultured chondrocytes. These findings suggest that CCN2 may regulate the proliferating and differentiation of chondrocytes by forming a complex with BMP-2 as a novel modulator of BMP signalling.

Key words: chondrocytes, CCN family 2/connective tissue growth factor (CCN2/CTGF), BMP signalling, BMP-2, endochondral ossification.

Abbreviations: E, embryonic day; ECM, extracellular matrix; ERK1/2, extracellular signal-regulated kinase 1/2; HA, influenza virus hemagglutinin; His, histidine; MAPK, mitogen-activated protein kinase; phospho, phosphorylation; rCCN2, recombinant CCN2 protein; WT, wild type.

INTRODUCTION

Endochondral ossification is initiated by the condensation of mesenchymal cells and the subsequent differentiation of them into chondrocytes within the condensates (1, 2). Chondrocytes proliferate and produce many kinds of extracellular matrix (ECM) molecules characteristic of cartilage, such as type II collagen, aggrecan, link proteins and hyaluronate (1, 2). Once embedded in ECM, these cells differentiate into pre-hypertrophic and hypertrophic chondrocytes (1, 2). Hypertrophic chondrocytes, in which cell growth is arrested, eventually mineralize the surrounding matrices, allowing the invasion of blood vessels and osteoblasts (1, 2). Finally, the cartilage is replaced by bone. In this differentiation process, a number of growth factors, such as transforming growth factor (TGF)- β (3), insulin-like growth factor (IGF, 4), bone morphogenetic proteins (BMPs, 5) and

CCN family 2/connective tissue growth factor (CCN2) have been implicated (6). Among them, CCN2 is highly expressed in the pre-hypertrophic region of growth plate (6). As a member of the CCN family, it consists of four distinct structural modules, i.e. insulin-like growth factor binding protein-like (IGFBP), von Willebrand type C repeat (VWC), thrombospondin type 1 repeat (TSP1) and carboxy-terminal cysteine knot (CT). Also, CCN2 promotes multiple steps of the endochondral ossification, such as proliferation, maturation and hypertrophy of chondrocytes (6, 7). In addition, we reported earlier that CCN2 functions to maintain the integrity of the cartilage tissues *in vivo* (8). These findings suggest that CCN2 plays a very important role in chondrocyte metabolism. In fact, it has been reported that *Ccn2*-deficient mice die soon after birth, as a result of, at least in part, severe skeletal abnormalities associated with impaired endochondral ossification (9). These and other findings indicate that CCN2 is an essential growth factor for regulation of the proliferation, maturation and hypertrophy of chondrocytes (7, 9). Recently, it was reported that CCN2 interacted with many growth factors critically

*To whom correspondence should be addressed. Tel: +81-86-235-6645, Fax: +81-86-235-6649, E-mail: takigawa@md.okayama-u.ac.jp

involved in cartilage metabolism, such as TGF- β , BMP-4 (10), and vascular endothelial growth factor (VEGF, 11) and that CCN2 modified the activity of each growth factor. Therefore, CCN2 may control the network of growth factors during endochondral ossification; and thus it may be called a 'signal conductor' with novel functions.

BMP-2 is also a multifunctional growth factor, and it was originally defined by its ability to induce ectopic bone and cartilage formation *in vivo* (12). Although it was reported that BMP-2 promoted the proliferation, maturation and hypertrophy of chondrocytes *in vitro* (5, 13, 14), newborn transgenic mice, in which Bmp-2 had been inactivated in a limb-specific manner, had normal skeletons (15). These findings suggest that other BMPs present in the developing limb can compensate for the loss of BMP-2. Until now, more than 30 BMP family members have already been described, and they have been classified into several subgroups according to their structural similarities (16). In particular, BMP-2 and BMP-4 are highly related molecules, and both molecules have potent bone-forming activity (17). These findings indicate that the functions of BMP-2 and BMP-4 are interchangeable during bone formation in the limb. In fact, it was reported that the loss of both BMP-2 and BMP-4 in a limb-specific manner resulted in a delay in cartilage development and in a severe impairment of osteogenesis (18). Furthermore, the BMP receptor type 1A (Bmpr1a), BMP receptor type 1B (Bmpr1b) double-deficient mice exhibited severe defects in chondrogenesis and osteogenesis (19). Taken together, these results suggest that BMP signalling is essential for endochondral ossification, and that BMP-2 and BMP-4 compensate each other to transduce sufficient BMP signalling to allow cartilage cells to differentiate.

Although it has been already reported that CCN2 interacts with BMP-4 and inhibits the action of BMP-4 in early embryonic patterning (7), investigation of the interaction of CCN2 with BMP-2 as well as BMP-4 may reveal the novel function of CCN2 in BMP signalling required for cartilage development. Therefore, we investigated whether or not CCN2 directly interacts with BMP-2 and examined the combinational effect of CCN2 with BMP-2 on chondrocyte proliferation and differentiation. In this study, we demonstrated that CCN2 directly interacted with BMP-2 and promoted CCN2/BMP-2-induced proteoglycan synthesis, whereas proliferation of chondrocytes was interfered with the combination. These findings suggest that CCN2 has both antagonistic effect and agonistic effect on BMP-2.

MATERIALS AND METHODS

Materials—Dulbecco's modified Eagle's medium (DMEM), α -modification of Eagle's medium (α MEM), and fetal bovine serum (FBS) were purchased from Nissui Pharmaceutical (Tokyo, Japan), ICN Biomedicals (Aurora, OH), and Cancera International (Rexdale, ON, Canada), respectively. Plastic dishes and multiwell plates were obtained from Greiner Bio-One (Frickenhausen, Germany). Hybond-N membrane and [α - 32 P]dCTP (specific activity: 110 TBq/mmol) were from GE Healthcare

UK (Little Chalfont, United Kingdom), and [35 S]sulfate (37 MBq/ml) was from PerkinElmer (Waltham, MA). Hyaluronidase and anti- β -actin were obtained from Sigma (St Louis, MO). Anti-phospho-extracellular signal-regulated kinase (ERK)1/2, and anti-phospho-p38 were from Promega (Madison, WI); and anti-ERK1/2, anti-p38, and anti-phospho-Smad1/5/8, from Cell Signaling Technology (Beverly, MA). Anti-BMP-2 was purchased from R & D Systems (Minneapolis, MN); and anti-HA, from Covance (Princeton, NJ). Anti-CCN2 serum was raised in rabbits, and recombinant CCN2 (rCCN2) was purified as previously reported (20). For binding assays and surface plasmon resonance (SPR) analysis, polyhistidine (His)-tagged rCCN2 and each of the four modules of the CCN2 were purchased from Biovendor (Heidelberg, Germany), or were produced by *Escherichia coli* harbouring the corresponding expression plasmids. Recombinant BMP-2 (rBMP-2) was kindly provided by Dr K. Sugama of Osteopharma (Osaka, Japan).

Animals—BalbC/129sv hybrid CCN2 $^{+/-}$ mice were crossbred to obtain wild-type (WT) and *Ccn2*-deficient mice, which were used at E18.5 (9). These mice were euthanized to obtain the rib cage for cell culture and the metatarsal bone with surrounding tissues for immunostaining. All mice were genotyped by using PCR. The Animal Committee of Okayama University Graduate School of Medicine, Dentistry, and Pharmaceutical Sciences approved all of the procedures.

Cell Culture—Cells of the human chondrosarcoma-derived cell line HCS-2/8 (21) were inoculated at a density of 4×10^4 cells/cm 2 into 96-well or 24-well multiplates containing DMEM supplemented with 10% FBS and were cultured at 37°C under 5% CO $_2$ in air. Primary cultures of chondrocytes isolated from the ventral half of the rib cages of E18.5 mouse embryos were prepared as described previously (22). The isolated chondrocytes were seeded at a density of 1×10^5 cells/cm 2 into 3.5 cm dishes in α MEM containing 10% FBS and were then cultured at 37°C under 5% CO $_2$ in air.

Western Blot Analysis—HCS-2/8 cells were transfected with a CCN2 expression plasmid with an HA-tag by using Fugene6 reagent (Roche, Basel, Switzerland). After 2 days, the cell lysate was collected, and immunoprecipitation was performed with anti-BMP-2 antibody. Then, the HA-tagged CCN2 was detected in the immunoprecipitated sample by western blotting by using an anti-HA antibody. Western blot analysis was performed as described previously (23).

Solid-Phase Binding Assay—A 96-well multiplate was pre-coated with rBMP-2 (0.3–10 μ g/ml) at 4°C overnight. Then, rCCN2 with a His-tag was added to each well, and incubation was carried out at 4°C for 6 h. After washing each well, we measured the optical absorbance (450 nm) representing the binding of CCN2 to BMP-2 by conducting a colorimetric assay using the anti-His antibody.

Immunohistochemistry—Mouse metatarsal bones with surrounding tissues were dissected and fixed in 10% formalin overnight at 4°C before being embedded in paraffin. Five micrometre sections were mounted on glass slides, deparaffinized and treated with hyaluronidase (25 mg/ml) for 30 min at room temperature. Immunohistochemistry was performed with a Histofine kit

(Nichirei; Tokyo, Japan) as described previously (23). Colour was developed with diaminobenzidine (DAB), and sections were counterstained with methyl green. The proliferative population of chondrocytes in growth cartilage tissues was determined using a commercial proliferating cell nuclear antigen (PCNA) staining kit (Zymed laboratories, Carlsbad, CA), following the manufacturer's instructions.

Evaluation of Proteoglycan Synthesis—Mouse costal chondrocytes or HCS-2/8 cells were grown to sub-confluence in 24-well multiplates containing α MEM or DMEM supplemented with 10% FBS, respectively. Thereafter, the medium was replaced with that containing 0.5% FBS and rCCN2, rBMP-2 or both. [35 S] sulfate (37 MBq/ml) dissolved in PBS was added to the culture at a final concentration of 370 kBq/ml at 5 h after the addition of these factors, and incubation was continued for another 17 h. After labelling, the cultures were digested with 1 mg/ml actinase E, and the radioactivity of the material precipitated with cetylpyridinium chloride was measured in a scintillation counter.

Northern Blot Analysis—Total RNAs were prepared by using ISOGEN reagent (Nippon Gene, Tokyo, Japan) from mouse costal chondrocytes stimulated with rCCN2, rBMP-2 or their combination for 6 h. Then, 10 μ g of total RNA was subjected to electrophoresis on a 1% formaldehyde-agarose gel and subsequently transferred onto Hybond-N filters (GE Healthcare). Northern blot analysis was performed as described previously (23). Specific PCR products of aggrecan cDNA and linearized plasmids containing mouse-type II collagen (22), type X collagen (9) and Runt domain transcription factor (Runx2/Cbfa1, 24) cDNAs were used as probes.

Surface Plasmon Resonance Spectroscopy—Specific interaction between CCN2 and BMP-2 was analysed by using a BIAcore X (GE HealthCare). rCCN2 coupling, blocking and regeneration of a CM5 chip were performed according to the manufacturer's protocol. rBMP-2 in HBS-EP buffer (10 mM HEPES, 0.15 M NaCl, 3 mM EDTA and 0.005% Tween 20; pH 7.4) at several concentrations was perfused at a flow rate of 10 μ l/min at 25°C over the control surface or a surface bearing immobilized CCN2, and the resonance changes were recorded. The response on the control surface was subtracted from that on the CCN2-conjugated surface. The dissociation constants (K_d) were determined by using BIA evaluation software.

Proliferation Assay—For measurement of cell proliferation, HCS-2/8 cells were inoculated into 96-well multiplates at a density of 1×10^4 /well, and then the cells were stimulated with rCCN2, rBMP-2 or their combination for 24 h. Thereafter, the proliferation of these cells was determined by conducting a TetraColor ONE assay according to the recommended protocol (Seikagaku Co. Tokyo, Japan). Briefly, 10 μ l of TetraColor ONE solution was added to 100 μ l of medium of each culture. After the incubation for up to 4 h at 37°C, the absorbance of culture medium was measured at a wavelength of 450 nm.

Statistical Analysis—Unless otherwise specified, all experiments were repeated at least twice, and similar results were obtained. Statistical analysis was performed by using Student's *t*-test.

RESULTS

Interaction of CCN2 with BMP-2 Through Its CT Domain—It has been reported that CCN2 directly binds to BMP-4 through its VWC module (10). Because not only BMP-4 but also BMP-2 plays an important role in chondrocyte proliferation and differentiation during endochondral ossification (13, 14), we investigated the involvement of CCN2 in BMP-2 signalling of chondrocytes. As shown in Fig. 1, we found that CCN2 interacted with BMP-2 similarly as with BMP-4. An HA epitope-tagged construct of full-length CCN2 was generated, and the protein was produced in HCS-2/8 cells. After 2 days, cell lysates were collected and immunoprecipitation was performed with anti-BMP-2 antibody in cell lysate in the presence or absence of rBMP-2. Western blot analysis of the immunoprecipitated samples was performed by using anti-HA antibody. As a result, HA-tagged CCN2 was detected only in the presence of rBMP-2 (Fig. 1A). In addition, to test whether CCN2 directly interacted with BMP-2, or not, we performed a solid-phase binding assay. As shown in Fig. 1B, CCN2 directly bound to BMP-2 in a BMP-2-dependent manner. Subsequently, a binding assay using each recombinant module protein of CCN2 was performed to determine which module was responsible for the binding to BMP-2. As shown in Fig. 1C, the CT module of CCN2 distinctly bound to BMP-2, whereas VWC and IGFBP modules slightly bound to it. To further verify if CT or amino-terminal module plays an important role in binding to BMP-2, we generated a N-terminal IGFBP-VWC and C-terminal TSP1-CT fragments and evaluated their binding ability. As shown in Fig. 1D, while both fragments significantly interacted with BMP-2, interaction of TSP1-CT fragment of CCN2 with BMP-2 was stronger than that of IGFBP-VWC fragment. These results indicate that not only the CT module, but also the IGFBP-VWC modules are responsible for the binding to BMP-2. Furthermore, the binding affinity of CCN2 for BMP-2 was determined by SPR analysis (BIAcore systems). Kinetic measurements using different concentrations of CCN2 yielded a K_d of 0.77 nM for BMP-2 (Fig. 1E). These data indicate that CCN2 can directly bind to BMP-2 through its CT domain.

Co-Localization of CCN2 with BMP-2 in Pre-Hypertrophic Region of the Growth Plate—Growth plate chondrocytes are horizontally organized into distinct zones. The zones reflect the sequential differentiation stages of chondrocyte proliferation, maturation and hypertrophy (Fig. 2A and B). In wild type mice, proliferative and pre-hypertrophic chondrocytes were stained with anti-PCNA antibody, which has been used as a marker for cell proliferation, but the immunoreactivity of PCNA was not observed in the hypertrophic chondrocytes therein (Fig. 2C). These findings suggest that not only proliferative chondrocytes, but also pre-hypertrophic chondrocytes, which are the major CCN2 producer in growth plate, retain proliferative activity. Because it was shown that CCN2 directly bound to BMP-2 *in vitro*, we investigated whether or not CCN2 was co-localized with BMP-2 in the growth plate using an immunohistochemical analysis with anti-CCN2 and anti-BMP-2 antibodies in E18.5 WT and *Ccn2*-deficient metatarsal growth plates. As shown in Fig. 2G and H,

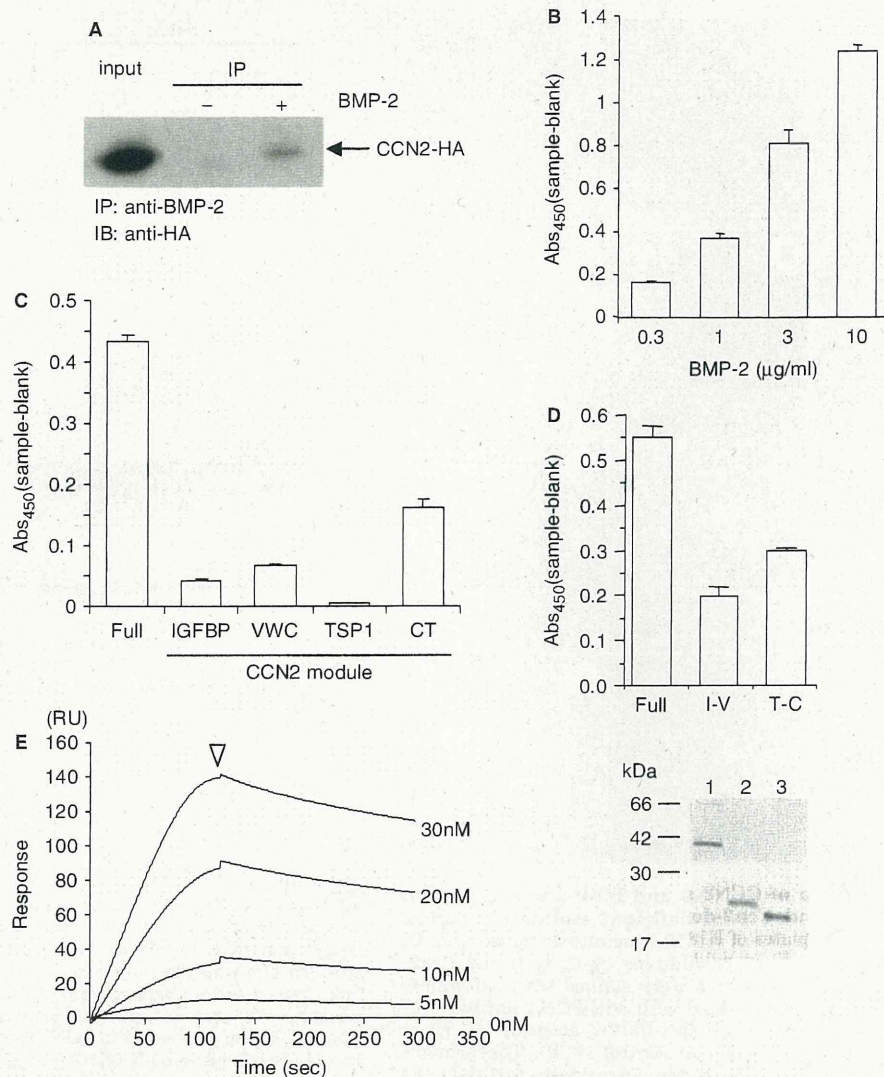


Fig. 1. Complex formation between CCN2 and BMP-2. (A) Western blot analysis of CCN2 binding to rBMP-2 after immunoprecipitation with anti-BMP-2. HCS-2/8 cells were inoculated at a density of 5×10^5 /well into a 6-well plate; and the next day, the cells were transfected with a CCN2 expression plasmid containing an HA tag. After 2 days, the cell lysates were collected and incubated with or without $1 \mu\text{g}$ rBMP-2 at 4°C overnight. Then, immunoprecipitation was performed with anti-BMP-2 antibody at 4°C . After 24 h, the immunocomplexes were captured by adding agarose-protein G beads. The beads were washed, and precipitates were subjected to SDS-PAGE and western blotting with anti-HA antibody. Representative results for total cell lysate (input) and treatment without rBMP-2 (-) and with rBMP-2 (+) are shown. The arrow indicates the signal for CCN2-HA. (B) Solid-phase binding assay for binding of full-length CCN2 to rBMP-2. Ninety-six multiplate wells pre-coated with different concentrations of rBMP-2 (0.3, 1, 3 and $10 \mu\text{g}/\text{ml}$) were incubated with $6 \times \text{His}$ -tagged rCCN2 ($500 \text{ ng}/\text{ml}$) at 4°C for 6 h. Total binding was determined by measuring immunoreactivity towards the His-tag. Background binding was determined by measuring the immunoreactivity towards the His-tagged CCN2 in the wells pre-coated with BSA at the same concentration of each rBMP-2. Data were calculated by the subtracting background binding

from the total binding. Data represents mean \pm SD of triplicate samples. (C) Solid-phase binding assay for measuring the binding of each CCN2 module to rBMP-2. CCN2 or its modules ($25 \mu\text{M}$) were incubated in the wells pre-coated with rBMP-2 at 4°C for 6 h. Bound proteins were determined under the same conditions as in 'B'. Data are presented as the mean \pm SD of triplicate samples. (D) Solid-phase binding assay for the evaluation of the binding of IGFBP-VWC or TSP1-CT fragment of CCN2 to rBMP-2. (Upper panel) Full-length CCN2, IGFBP-VWC or TSP1-CT fragment ($1 \mu\text{g}/\text{ml}$) was incubated in the wells pre-coated with rBMP-2 ($3 \mu\text{g}/\text{ml}$) at 4°C for 6 h. Bound proteins were determined under the same conditions as in 'B'. Data are presented as the mean \pm SD of triplicate samples. (Lower panel) Recombinant full-length CCN2, IGFBP-VWC and TSP1-CT fragment were separated by SDS-PAGE and visualized by coomassie brilliant blue (CBB) staining. (E) Determination of the binding affinity of rBMP-2 for CCN2 by SPR analysis. Four different concentrations of rBMP-2 ranging between 5 nM and 30 nM were passed through the immobilized CCN2 on the CM5 sensor chip (Time 0s), and kinetic experiments were performed. After the rBMP-2 flow was stopped (arrowhead), dissociation was monitored by a decrease in the resonance units.

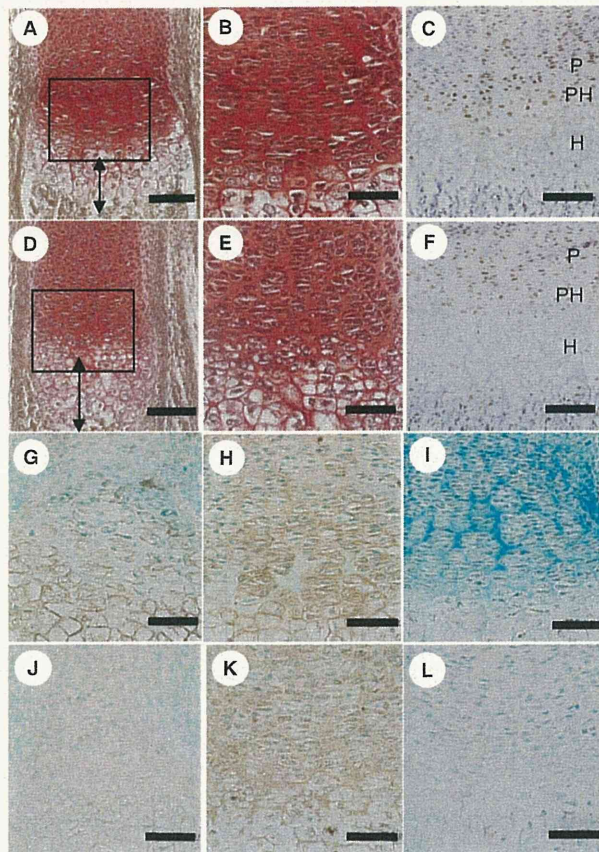


Fig. 2. Co-localization of CCN2 and BMP-2 in the growth plate of wild-type and *Ccn2*-deficient metatarsal bones. Sections of the growth plates of E18.5 metatarsal bone (A, B, D, E, G–L) and femur (C, F) in wild-type (A–C, G–I) and *Ccn2*-deficient (D–F, J–L) littermates were stained with safranin-O (A, B, D, E), and immunostained with anti-PCNA antibody (C, F), anti-CCN2 antibody (G, J), anti-BMP-2 antibody (H, K) or normal rabbit IgG as a negative control (I, L). The primary antibodies were visualized by immunoperoxidase, and then the sections were counterstained with methyl green (G–L) or hematoxylin (C, F). Panels 'A' and 'D' are low-power magnification views of the growth plate, and panels 'B, G–I' and 'E, J–L' show high-power magnification of the area delimited by black square in 'A' and 'D', respectively. Bidirectional arrows indicate the length of the hypertrophic zones (A, D). In the wild type, immunostaining with PCNA was detected from proliferative to pre-hypertrophic zone (C), and both CCN2 and BMP-2 were mainly localized in the pre-hypertrophic zone of the growth plate (G, H). In the *Ccn2*-deficient mice, signals for immunoreactivity of PCNA were decreased compared with wild type (F), and CCN2 immunostaining was not detected (J). Signals for immunoreactivity to BMP-2 were located in the proliferative zone (K). Bars in 'A' and 'D' and in 'B, C, E, F and G–L' represent 100 μ m and 50 μ m, respectively.

both CCN2 and BMP-2 were localized in pre-hypertrophic region of the growth plate, thus suggesting that CCN2 might interact with BMP-2 *in vivo*. On the other hand, as also shown in Fig. 2D–F, J–L, and consistent with previous studies (9), an enlarged hypertrophic zone and reduced PCNA signal and safranin-O staining were seen in the growth plate in *Ccn2*-deficient compared with

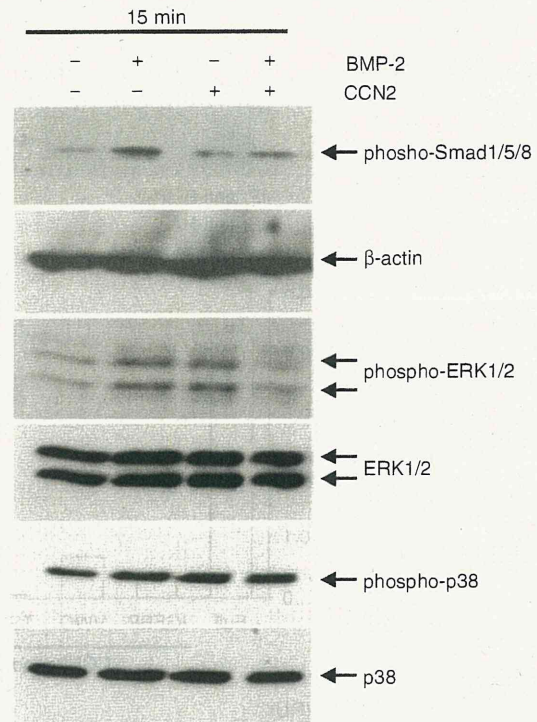


Fig. 3. Combinational effect of CCN2 and BMP-2 on the activation of Smad1/5/8 and MAPK pathways in mouse chondrocytes. After the first passage, mouse chondrocytes were cultured in 3.5 cm dishes until they had become sub-confluent. Then, the cells were stimulated with 50 ng/ml rBMP-2, 100 ng/ml rCCN2 or the combination of CCN2 (100 ng/ml) and rBMP-2 (50 ng/ml) for 15 min. The mixture of CCN2 with BMP-2 was prepared 2 h before stimulation and was kept on ice to allow hetero complex formation. Cell lysates were collected, and western blot analysis was performed with anti-phospho-Smad1/5/8, anti- β -actin, anti-phospho-ERK1/2, anti-ERK1/2, anti-phospho-p38 and anti-p38 antibodies. The band of phospho-Smad1/5/8 was increased in cells treated with rBMP-2, and the bands of both phospho-ERK1/2 and phospho-p38 were increased in the cells treated with rCCN2 or rBMP-2 after 15 min of treatment. Note that combination of CCN2 and BMP-2 decreased the activation of phospho-Smad1/5/8 and phospho-ERK1/2 but not that of phospho-p38.

that in WT littermates; and as expected, immunoreactivity for CCN2 was not detected (Fig. 2J). Signals indicating immunoreactivity for BMP-2 were detected in chondrocytes in the proliferative cell layer, but not in the pre-hypertrophic zone (Fig. 2K). This pattern of BMP-2 distribution in the *Ccn2*-deficient mice was significantly altered from that in the WT mice. These findings suggest that CCN2 regulates the localization of BMP-2 during endochondral ossification.

Combination of CCN2 and BMP-2 Modulates the CCN2 or BMP-2 Signalling in Chondrocytes—Because CCN2 interacted with BMP-2 *in vitro* and co-localized with BMP-2 *in vivo*, we tested whether the combination of CCN2 and BMP-2 modulated CCN2 or BMP-2 signalling in chondrocytes, or not. As shown in Fig. 3, we performed western blot analysis of mouse costal

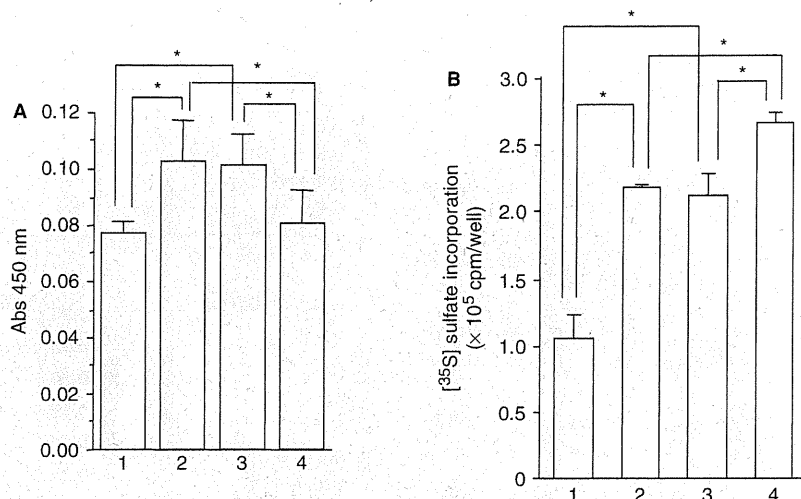


Fig. 4. Combinational effect of CCN2 and BMP-2 on the proliferation and differentiation of HCS-2/8 cells. (A) Effect of the combination of CCN2 and BMP-2 on the proliferation of HCS-2/8 cells. HCS-2/8 cells in DMEM containing 10% FBS were inoculated at a density of 1×10^4 /well into the wells of a 96-well multiplate and cultured for 24 h. Then, the cells were stimulated with final concentrations of 50 ng/ml rBMP-2, 100 ng/ml rCCN2 or the combination of CCN2 (100 ng/ml) and BMP-2 (50 ng/ml) for 24 h. The mixture of CCN2 with BMP-2 was prepared and kept on ice for 2 h before the stimulation. The proliferation assay was performed as described in 'MATERIALS AND METHODS' section. Column 1 represents cells cultured with PBS (control); column 2, those with rBMP-2; column 3, those with rCCN2; and column 4, those with the combination of both. Asterisks indicate significant differences ($P < 0.05$) between values indicated by the

brackets. Each column shows the mean value and SD of the results from 8 wells. (B) Effect of the combination of CCN2 and BMP-2 on proteoglycan synthesis in HCS-2/8 cells. Once HCS-2/8 cells had reached sub-confluence, they were treated with PBS (column 1), rBMP-2 (column 2), rCCN2 (column 3) or both (column 4) for 22 h at 37°C. At 5 h after the addition of these factors, [³⁵S]sulfate was added to the cultures; and radioactivity incorporated into proteoglycans was measured 17 h later. Values represent the means \pm SD of four independent cultures. Column 1 represents cells cultured with PBS (control), column 2, those with rBMP-2; column 3, those with rCCN2; and column 4, those with both CCN2 and BMP-2. Asterisks indicate significant differences ($P < 0.05$) between values indicated by the brackets.

chondrocytes stimulated with rCCN2, rBMP-2 or their combination for 15 or 30 min by using anti-phospho-Smad1/5/8, anti-phospho-ERK1/2 and anti-phospho-p38 antibodies. The levels of Smad1/5/8 and ERK1/2 phosphorylation were increased by 50 ng/ml rBMP-2 and the phosphorylation of ERK1/2 was induced by 100 ng/ml rCCN2. However, the degree of their phosphorylation by the combination of rCCN2 and rBMP-2 was rather decreased compared with that by either factor alone (Fig. 3). Similar results were obtained in HCS-2/8 cells (data not shown). On the other hand, phospho-p38 levels were not affected by the combination of rCCN2 and rBMP-2. After 30 min of stimulation, no effect on Smad1/5/8, ERK1/2 or p38 phosphorylation was detected (data not shown). These findings suggest that the co-presence of CCN2 and BMP-2 modulates BMP-2 or CCN2 signaling in chondrocytes.

Effect of Combination of CCN2 and BMP-2 on the Proliferation and Differentiation of HCS-2/8 Cells—Because the combination of CCN2 and BMP-2 modulated CCN2 or BMP-2 signalling, we next investigated the biological significance of the combination of CCN2 and BMP-2 in HCS-2/8 cells. HCS-2/8 cells have retained the mature chondrocytic phenotype during a number of passages, and their responsiveness to growth factors and cytokines is similar to that of primary chondrocytes (21). Therefore, we first studied the effect of the combination

of CCN2 and BMP-2 on the proliferation of the cells. As shown in Fig. 4A, rCCN2 or rBMP-2 tested alone stimulated the proliferation of the cells, but their combination showed no stimulatory effect. Second, to investigate the effect of the combination of CCN2 and BMP-2 on the differentiation of HCS-2/8 cells, we evaluated proteoglycan synthesis, which is a good marker of differentiated chondrocytes, in the cells stimulated by the combination of rCCN2 and rBMP-2. As shown in Fig. 4B, either rBMP-2 or rCCN2 alone stimulated the proteoglycan synthesis, which was consistent with previous studies (13, 14, 25). Interestingly, when the combination of CCN2 and BMP-2 was added to the culture of HCS-2/8 cells, proteoglycan synthesis was additively increased. These findings suggest that the combination of CCN2 and BMP-2 collaboratively promoted the differentiation of HCS-2/8 cells but that the proliferation was rather interfered with by the combination.

Effect of Combination of CCN2 and BMP-2 on the Expression of Chondrocyte Marker Genes and Differentiation of Mouse Primary Chondrocytes—To clarify in detail the differentiation of chondrocytes stimulated with the combination of CCN2 and BMP-2, we performed northern blot analysis of various cartilage differentiation markers, i.e. type II collagen, aggrecan, type X collagen and Runx2/Cbfa1. As shown in Fig. 5A,

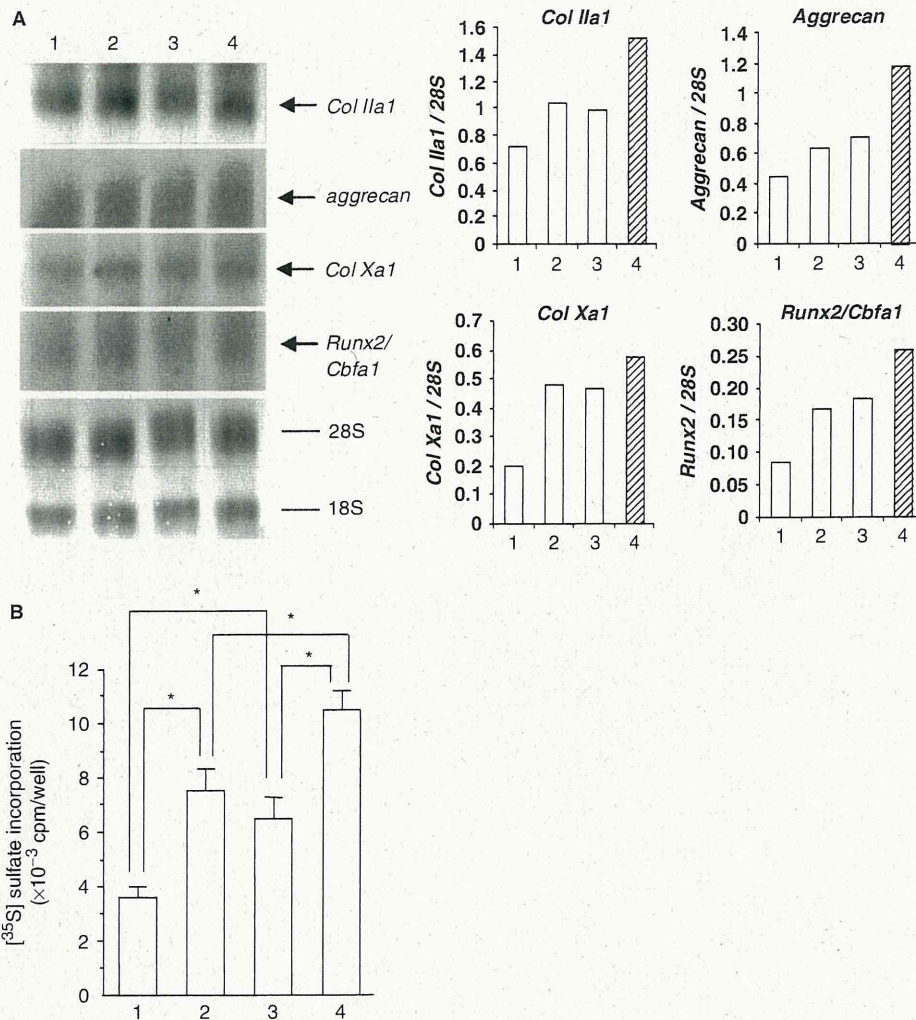


Fig. 5. Combinational effect of CCN2 and BMP-2 on expression of the differentiated phenotype of chondrocytes in mouse chondrocytes in culture. (A) Northern blot analysis of the expression of type II collagen, aggrecan, type X collagen and Runx2/Cbfa1 in mouse chondrocytes. Mouse primary chondrocytes were re-plated into 6 cm dishes, and they were then cultured until they had reached confluence. Thereafter, the medium was replaced with serum-free medium containing rBMP-2 (50 ng/ml), rCCN2 (100 ng/ml) or the combination of CCN2 and BMP-2; and total RNA was prepared 6 h later. Northern blot analysis was performed as described in 'MATERIALS AND METHODS section'. Hybridization signals of cartilage marker genes in the autoradiogram and methylene blue-stained rRNA on the same membrane are displayed. Representative results of treatment with PBS (lane 1), rBMP-2

(lane 2), rCCN2 (lane 3) and their combination (lane 4) are shown. The amounts of cartilage marker genes were normalized to the amounts of 28S rRNA. (B) Effect of the combination of CCN2 and BMP-2 on proteoglycan synthesis in mouse chondrocytes. After mouse chondrocytes of passage 1 had reached subconfluence, the medium was replaced with α MEM containing 0.5% FBS and PBS (lane 1), rBMP-2 (50 ng/ml, lane 2), rCCN2 (100 ng/ml, lane 3) or the combination of CCN2 and BMP-2 (lane 4); and incubation was further continued for 22 h at 37°C. After 5 h of stimulation, [³⁵S]sulfate was added to the cultures; and radioactivity incorporated into proteoglycans was then measured. Values represent means \pm SD of four cultures. Asterisks indicate significant differences ($P < 0.05$) between values indicated by the brackets.

the expression of type II collagen and aggrecan, which are good markers of mature chondrocytes, was promoted by the combination of rCCN2 and rBMP-2 better than that by each factor alone. In addition, the combination of rCCN2 and rBMP-2 also stimulated the expression of type X collagen and Runx2/Cbfa1, which are markers of hypertrophic chondrocytes, to a greater degree than each factor alone. Furthermore, to confirm whether or not combination of CCN2 and BMP-2 stimulated

proteoglycan synthesis in a synergistic or additive manner, we treated mouse costal chondrocyte cultures with the combination of rCCN2 and rBMP-2 (Fig. 5B). As shown in Fig. 5B, the combination of rCCN2 and rBMP-2 increased proteoglycan synthesis additively, consistent with the result in Fig. 4B. These results suggest that the combination of CCN2 and BMP-2 stimulates chondrocyte differentiation better than CCN2 or BMP-2 alone.

DISCUSSION

In this study, we demonstrated that CCN2 directly interacted with BMP-2. It was previously reported that CCN2 directly bound BMP-4 through its VWC domain and that CCN2 inhibited BMP-4 action (10). The same study also showed, by western blot analysis, that the binding of BMP-4 to CCN2 could be competed by an excess of BMP-2, which suggests that CCN2 also binds to BMP-2 through the same domain (10). This VWC domain is 80% homologous to chordin, which is a BMP antagonist in terms of the cysteine residues (26). Therefore, this finding indicates that CCN2 may be a novel BMP antagonist. In this study, we investigated whether CCN2 directly binds to BMP-2 and functions as a BMP-2 antagonist, or not. BMP-2 has various effects on cartilage metabolism (13, 14). It was reported that BMP-2 stimulated the proliferation, maturation and hypertrophy of chondrocytes *in vitro* (13, 14), but apparently contradictory results were obtained in an *in vivo* study using genetically modified mice (15–18). These findings suggest that there are many factors regulating BMP signalling *in vivo*. In the solid-phase binding assay using each recombinant module protein, we showed that CCN2 bound to BMP-2 mainly through its CT module and partially through its IGFBP and VWC modules (Fig. 1C). In addition, we confirmed that binding of TSP1-CT fragment to BMP-2 was more prominent than that of IGFBP-VWC fragment (Fig. 1D). Inkson *et al.* reported that [CXXXCXC] and [CCXXC] motifs, which are typical chordin cysteine-rich (CR) sequences, have been conserved in the VWC domain of CCN2 binding to BMPs (26). It should be noted that reversed [CXCXXXC] and [CXXCC] motifs are present in the CT module of CCN2. Therefore, BMP-2 may bind to CCN2 probably via these sequences in the CT module as well.

The crystal structure of CCN2 is still unknown. Previously, we raised several monoclonal antibodies against CCN2 by using a recombinant full-length CCN2 protein as an immunogen, and located the epitopes in the module in CCN2. As a result, we found that two of five monoclonal antibodies recognized the VWC module (27). These results indicate the strong antigenicity of the VWC module and suggest that this module is exposed on the molecular surface. In addition, it has been suggested that CCN2 forms a dimer *via* the CT domain (28), and that CT domain also directly interacts with ECM proteins, such as fibronectin and heparan sulfate (28, 29). Under the condition that CCN2 is overexpressed in the cells, the binding of BMP-2 to the CT domain may not occur, because this domain is engaged in the dimerization of CCN2 or interacts with ECM. Thus, the VWC module may be more accessible than the CT module. If so, the VWC module may be a major interface for CCN2-BMP interaction. Nevertheless, we showed the binding of CT module to BMP-2 and the modest binding of IGFBP and VWC modules in this binding study; hence, binding of VWC module to BMP-2 may require the collaboration of the IGFBP module to confer the full binding activity. In fact, we showed that the amount of total binding of TSP1-CT and IGFBP-VWC fragments to BMP-2 was comparable with the binding of full-length CCN2. These findings suggest that both IGFBP-VWC and CT

domains contribute to the interaction of CCN2 with BMP-2.

BMPs transduce signals by binding to heteromeric complexes of type I and type II serine/threonine kinase receptors. The binding of BMPs to the receptor complex results in the phosphorylation of intracellular Smads, which then are translocated to the nucleus, where they regulate the transcription of the target genes (5, 16, 30). On the other hand, it has been also reported that BMPs transduce signals by the activation of mitogen-activated protein kinase (MAPK) pathways (5, 30) and that the activation of MAPK, especially the p38 pathway, plays an important role in chondrocyte differentiation (31). In addition, the expression of the Runx2/Cbfa1 gene, which induces cartilage hypertrophy, is up-regulated by rBMP-2 treatment (30, 32). In this study, we showed that phosphorylation of Smad1/5/8 induced by BMP-2 treatment was inhibited by the co-presence of CCN2. Furthermore, the activation of ERK1/2 and p38 MAPK pathways was induced by BMP-2, but phosphorylation of ERK1/2 was dramatically decreased by the co-presence of CCN2 with BMP-2 in chondrocytes (Fig. 3). These results suggest that CCN2 binds to BMP-2 and regulates the BMP signalling pathways. Typical antagonists, such as noggin, chordin and follistatin, bind to BMPs and prevent them from interacting with their receptors (30, 33). The major difference between CCN2 and other BMP antagonists is that CCN2 itself is a growth factor and activates the signalling to the nucleus. We reported that the phosphorylation of ERK1/2 was involved in chondrocyte proliferation and that the phosphorylation of p38 MAPK was involved in chondrocyte differentiation induced by rCCN2 (34). In fact, we showed presently that the co-presence of CCN2 with BMP-2 inhibited chondrocyte proliferation and promoted proteoglycan synthesis in HCS-2/8 cells (Fig. 4). In addition, this co-presence increased the gene expression of chondrocyte differentiation markers, such as type II collagen, aggrecan and type X collagen, and promoted proteoglycan synthesis in mouse chondrocytes as well as in HCS-2/8 cells (Fig. 5). Also, we reported that PD98059, which is a specific MEK inhibitor, blocked chondrocyte proliferation and stimulated proteoglycan synthesis in HCS-2/8 cells (34). Considering these findings, a decrease in ERK1/2 signalling caused by the complex formation of CCN2 with BMP-2 may lead to the inhibition of the proliferation and promotion of the differentiation of chondrocytes. The expression of type X collagen mRNA, which is a marker of chondrocyte hypertrophy, was also increased by the combination of CCN2 and BMP-2 treatment, in spite of the decreased Smad1/5/8 phosphorylation representing the classical BMP signalling. However, we also showed that the gene expression of Runx2/Cbfa1 was increased by the combination of CCN2 and BMP-2 treatment of chondrocytes (Fig. 5). Therefore, we propose that the level of expression of type X collagen mRNA was increased due to the up-regulation of Runx2/Cbfa1 induced by stimulation from the combination of CCN2 and BMP-2. Taken together, these findings indicate that CCN2 interacted with BMP-2 to inhibit chondrocyte proliferation and to promote differentiation, thus suggesting that CCN2 modulates not only BMP signalling but also its own signalling to regulate the chondrocyte

proliferation and differentiation as a 'signal conductor'. We conclude that CCN2 has both antagonistic effect and agonistic effect of BMP-2 during endochondral ossification.

FUNDING

This work was supported in part by the programs Grants-in-Aid for Medical and Dental Postgraduate Education (to A.M.) and Exploratory Research (to M.T.) of the Ministry of Education, Culture, Sports, Science, and Technology, Japan, and Grants-in-Aid for Scientific Research (S) (to M.T.) and (C) (to S.K.) from Japan Society for the Promotion of Sciences.

ACKNOWLEDGEMENT

We thank Drs Takako Hattori and Harumi Kawaki for their helpful suggestions and are also grateful to Yoko Tada for secretarial assistance.

CONFLICT OF INTEREST

None declared.

REFERENCES

- Zelzer, E. and Olsen, B.R. (2003) The genetic basis for skeletal diseases. *Nature* **423**, 343–348
- Shimizu, H., Yokoyama, S., and Asahara, H. (2007) Growth and differentiation of the developing limb bud from the perspective of chondrogenesis. *Develop. Growth Differ.* **49**, 449–454
- Redini, F., Galera, P., Mauviel, A., Loyau, G., and Pujol, J.P. (1988) Transforming growth factor β stimulates collagen and glycosaminoglycan biosynthesis in cultured rabbit articular chondrocytes. *FEBS Lett.* **234**, 172–176
- Trippel, S.B. (1992) Role of insulin-like growth factors in the regulation of chondrocytes in *Biological Regulation of the Chondrocytes* (Adolphe, M., ed.) pp. 161–190, CRC Press, Boca Raton, FL
- Yoon, B.S. and Lyons, K.M. (2004) Multiple functions of BMPs in chondrogenesis. *J. Cell. Biochem.* **93**, 93–103
- Kubota, S. and Takigawa, M. (2007) Role of CCN2/CTGF/Hcs24 in bone growth. *Int. Rev. Cytol.* **257**, 1–41
- Nakanishi, T., Nishida, T., Shimo, T., Kobayashi, K., Kubo, T., Tamatani, T., Tezuka, K., and Takigawa, M. (2000) Effects of CTGF/Hcs24, a product of a hypertrophic chondrocyte-specific gene, on the proliferation and differentiation of chondrocytes in culture. *Endocrinology* **141**, 264–273
- Nishida, T., Kubota, S., Kojima, S., Kuboki, T., Nakao, K., Kushibiki, T., Tabata, Y., and Takigawa, M. (2004) Regeneration of defects in articular cartilage in rat knee joints by CCN2 (connective tissue growth factor). *J. Bone Miner. Res.* **19**, 1308–1319
- Ivkovic, S., Yoon, B.S., Popoff, S.N., Safadi, F.F., Libuda, D.E., Stephenson, R.C., Daluiski, A., and Lyons, K.M. (2003) Connective tissue growth factor coordinates chondrogenesis and angiogenesis during skeletal development. *Development* **130**, 2779–2791
- Abreu, J.G., Ketpura, N.I., Reversade, B., and de Robertis, E.M. (2002) Connective-tissue growth factor (CTGF) modulates cell signalling by BMP and TGF- β . *Nat. Cell Biol.* **4**, 599–604
- Inoki, I., Shiomi, T., Hashimoto, G., Enomoto, H., Nakamura, H., Makino, K., Ikeda, E., Takata, S., Kobayashi, K., and Okada, Y. (2002) Connective tissue growth factor binds vascular endothelial growth factor (VEGF) and inhibits VEGF-induced angiogenesis. *FASEB J.* **16**, 219–221
- Wozney, J.M. (1989) Bone morphogenetic proteins. *Prog. Growth Factor Res.* **1**, 267–280
- Valcourt, U., Ronzière, M.-C., Winkler, P., Rosen, V., Herbage, D., and Mallein-Gerin, F. (1999) Different effects of bone morphogenetic proteins 2, 4, 12, and 13 on the expression of cartilage and bone markers in the MC615 chondrocyte cell line. *Exp. Cell Res.* **251**, 264–274
- Shukunami, C., Ohta, Y., Sakuda, M., and Hiraki, Y. (1998) Sequential progression of the differentiation program by bone morphogenetic protein-2 in chondrogenic cell line ATDC5. *Exp. Cell Res.* **241**, 1–11
- Tsuji, K., Bandyopadhyay, A., Harfe, B.D., Cox, K., Kakar, S., Gerstenfeld, L., Einhorn, T., Tabin, C.J., and Rosen, V. (2006) BMP2 activity, although dispensable for bone formation, is required for the initiation of fracture healing. *Nat. Genet.* **38**, 1424–1429
- von Bubnoff, A. and Cho, K.W. (2001) Intracellular BMP signaling regulation in vertebrates: pathway or network? *Dev. Biol.* **239**, 1–14
- Tsuji, K., Cox, K., Bandyopadhyay, A., Harfe, B.D., Tabin, C.J., and Rosen, V. (2008) BMP4 is dispensable for skeletogenesis and fracture-healing in the limb. *J. Bone Joint Surg. Am.* **90**, 14–18
- Bandyopadhyay, A., Tsuji, K., Cox, K., Harfe, B.D., Rosen, V., and Tabin, C.J. (2006) Genetic analysis of the roles of BMP2, BMP4, and BMP7 in limb patterning and skeletogenesis. *PLoS Genet.* **2**, 2116–2130
- Yoon, B.S., Ovchinnikov, D.A., Yoshii, I., Mishina, Y., Behringer, R.R., and Lyons, K.M. (2005) *Bmpr1a* and *Bmpr1b* have overlapping functions and are essential for chondrogenesis in vivo. *Proc. Natl. Acad. Sci. USA.* **102**, 5062–5067
- Nishida, T., Nakanishi, T., Shimo, T., Asano, M., Hattori, T., Tamatani, T., Tezuka, K., and Takigawa, M. (1998) Demonstration of receptors specific for connective tissue growth factor on a human chondrocytic cell line (HCS-2/8). *Biochem. Biophys. Res. Commun.* **247**, 905–909
- Takigawa, M., Tajima, K., Pan, H.-O., Enomoto, M., Kinoshita, A., Suzuki, F., Takano, Y., and Mori, Y. (1989) Establishment of a clonal human chondrosarcoma cell line with cartilage phenotypes. *Cancer Res.* **49**, 3996–4002
- Nishida, T., Kawaki, H., Baxter, R.M., Deyoung, R.A., Takigawa, M., and Lyons, K.M. (2007) CCN2 (connective tissue growth factor) is essential for extracellular matrix production and integrin signaling in chondrocytes. *J. Cell Commun. Signal.* **1**, 45–58
- Nishida, T., Kubota, S., Fukunaga, T., Kondo, S., Yosimichi, G., Nakanishi, T., Takano-Yamamoto, T., and Takigawa, M. (2003) CTGF/Hcs24, hypertrophic chondrocyte-specific gene product, interacts with perlecan in regulating the proliferation and differentiation of chondrocytes. *J. Cell. Physiol.* **196**, 265–275
- Yamaai, T., Nakanishi, T., Asano, M., Nawachi, K., Yosimichi, G., Ohyama, K., Komori, T., Sugimoto, T., and Takigawa, M. (2005) Gene expression of connective tissue growth factor (CTGF/CCN2) in calcifying tissues of normal and *cbfa1*-null mutant mice in late stage of embryonic development. *J. Bone Miner. Metab.* **23**, 280–288
- Nishida, T., Kubota, S., Nakanishi, T., Kuboki, T., Yosimichi, G., Kondo, S., and Takigawa, M. (2002) CTGF/Hcs24, a hypertrophic chondrocyte-specific gene product, stimulates proliferation and differentiation, but not hypertrophy of cultured articular chondrocytes. *J. Cell. Physiol.* **192**, 55–63
- Inkson, C.A., Ono, M., Kuznetsov, S.A., Fisher, L.W., Gehron Robey, P., and Young, M.F. (2008) TGF- β 1 and WISP-1/CCN4 can regulate each other's activity to cooperatively control osteoblast function. *J. Cell. Biochem.* **104**, 1865–1878

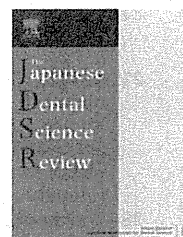
27. Minato, M., Kubota, S., Kawaki, H., Nishida, T., Miyauchi, A., Hanagata, H., Nakanishi, T., Takano-Yamamoto, T., and Takigawa, M. (2004) Module-specific antibodies against human connective tissue growth factor: utility for structural and functional analysis of the factor as related to chondrocytes. *J. Biochem.* **135**, 347–354
28. Brigstock, D.R., Steffen, C.L., Kim, G.Y., Vegunta, R.K., Diehl, J.R., and Harding, P.A. (1997) Purification and characterization of novel heparin-binding growth factors in uterine secretory fluids: identification as heparin-regulated Mr 10,000 forms of connective tissue growth factor. *J. Biol. Chem.* **272**, 20275–20282
29. Hoshijima, M., Hattori, T., Inoue, M., Araki, D., Hanagata, H., Miyauchi, A., and Takigawa, M. (2006) CT domain of CCN2/CTGF directly interacts with fibronectin and enhances cell adhesion of chondrocytes through integrin $\alpha 5 \beta 1$. *FEBS Lett.* **580**, 1376–1382
30. Tsumaki, N. and Yoshikawa, H. (2005) The role of bone morphogenetic proteins in endochondral bone formation. *Cytokine Growth Factor Rev.* **16**, 279–285
31. Stanton, L.-A., Underhill, T. M., and Beier, F. (2003) MAP kinases in chondrocyte differentiation. *Dev. Biol.* **263**, 165–175
32. de Crombrughe, B., Lefebvre, V., and Nakashima, K. (2001) Regulatory mechanisms in the pathways of cartilage and bone formation. *Curr. Opin. Cell Biol.* **13**, 721–727
33. Balemans, W. and Vau Hul, W. (2002) Extracellular regulation of BMP signaling in vertebrates: a cocktail of modulators. *Dev. Biol.* **250**, 231–250
34. Yosimichi, G., Kubota, S., Nishida, T., Kondo, S., Yanagita, T., Nakao, K., Takano-Yamamoto, T., and Takigawa, M. (2006) Roles of PKC, PI3K and JNK in multiple transduction of CCN2/CTGF signals in chondrocytes. *Bone* **38**, 853–863



available at www.sciencedirect.com



journal homepage: www.elsevier.com/locate/jdsr



Review

The effect of growth factors for bone augmentation to enable dental implant placement: A systematic review

Kengo Shimono, Masamitsu Oshima, Hikaru Arakawa, Aya Kimura, Kumiko Nawachi, Takuo Kuboki *

Oral Rehabilitation and Regeneration Medicine, Okayama University Graduate School of Medicine, Dentistry and Pharmaceutical Sciences, Okayama 700-8525, Japan

Received 17 March 2009; received in revised form 13 October 2009; accepted 27 October 2009

KEYWORDS

Growth factors;
Dental implant;
Bone augmentation;
Systematic review;
Clinical trial

Summary This systematic review assessed the potential benefits of growth factors for bone augmentation prior to the placement of dental implants in human.

A systematic online review of the Medline database, using the PubMed search machine was performed between 1966 and November 2008 by entering the MeSH terms. The primary outcome of the included studies was bone regeneration of localized alveolar ridge defects.

The initial search identified 119 papers from the electronic database. This review produced seven eligible papers that reported on bone augmentation with recombinant human Bone Morphogenetic Protein-2 (rhBMP-2), recombinant human Platelet-Derived Growth Factor (rhPDGF) and Plasma-Rich Growth Factor (PRGF). The rhBMP-2 affected local bone augmentation with increasing volume for higher doses. Both rhPDGF and PRGF showed a positive effect in favor of the growth factor.

Differing levels and quantity of evidence were noted to be available for the growth factors evaluated, revealing that rhBMP-2, rhPDGF, and PRGF may stimulate local bone augmentation to various conditions. Especially the potential of rhBMP-2 is supportive. However, the confined number of investigators using these techniques and the low number of patient treatments reported in the literature, the generalizability of this approach is limited at this time.

© 2009 Japanese Association for Dental Science. Published by Elsevier Ireland. All rights reserved.

Contents

| | |
|--|----|
| Introduction | 44 |
| Material and methods | 44 |
| Study selection | 44 |
| The inclusion and exclusion criteria | 44 |
| The data extraction | 45 |

* Corresponding author. Tel.: +81 86 235 6680; fax: +81 86 235 6684.
E-mail address: kuboki@md.okayama-u.ac.jp (T. Kuboki).

| | |
|---|----|
| Result | 45 |
| The study characteristics | 45 |
| Bone height increase/defect size decrease | 45 |
| New bone formation | 45 |
| Safety | 49 |
| Discussion | 49 |
| Acknowledgements | 51 |
| References | 51 |

Introduction

Dental implants are the most innovative and superior treatment in dentistry, and are widely used for a variety of cases. Most of the techniques that are used are evidence-based and predictable. However, in many cases, the intended implant site is inappropriate due to the poor bone quality or to an insufficient quantity of bone. An insufficient alveolar ridge height is often related to the proximity of the implant site to other anatomical structures, i.e., the maxillary sinus or the mandibular canal.

In order to overcome some of these difficulties, autogenous bone grafts taken from the chin, the ramus of the mandible, or the iliac crest of the same patient have historically been the standard for alveolar reconstruction, specifically, due to their osteoconductive, osteoinductive, and lack of immunogenic properties. However, the adverse events and complications, such as infection, pain, sensory loss, and hematoma formation at the donor site, occur frequently upon autogenous bone graft treatment. In addition, a donor site with a sufficient quantity of bone is not always available. Allograft bones, bones taken from a different person and processed and managed by a tissue bank or commercial supplier, have often been substituted. However, this method also has limitations, including an inconsistent osteoinductive activity, unfavorable host immune responses [1], a delayed resorption, and a risk for prion and virus transmissions [2,3].

An ideal bone graft in implant dentistry should have the following properties: it should be biomimetic; it should have the ability to induce differentiation of the appropriate cells (i.e., endothelial and osteoblastic cells) for the formation of new bone; it should be easily synthesized or produced, rather than extracted from allograft materials (to eliminate all risks of disease transmission); it should be easily and quickly resorbed as the osteogenic response occurs; it should have no immune-provoking properties; it should be easily transported and stored; it should be reasonably cost-effective; it should be capable of achieving consistent and predictable results without being affected by different level of technical ability of the clinician.

In order to meet these demands, dental research has focused on the use of bioactive molecules to induce local bone formation. Since the various growth factors that have an effect on the bone regeneration have been discovered, the number of related studies has increased substantially. In particular, the factors recombinant human Bone Morphogenetic Protein-2 (rhBMP-2) [4–7] and recombinant human Platelet-Derived Growth Factor (rhPDGF) [8–10] have been shown to induce bone formation at the compromised sites in a variety of experimental and clinical situations. These factors

have also been approved by the U.S. Food and Drug Administration (FDA) for use in dentistry.

To date, there is only limited evidence to support the application of growth factors for local bone augmentation in dentistry. The aim of this systematic review was to summarize the current literature that describes the use of growth factors in conjunction with dental implants.

Material and methods

Study selection

We conducted an electronic search of the Medline database, using the PubMed search machine, for the relevant selection of studies by entering the following MeSH terms: "Inter-cellular Signaling Peptides and Proteins;" and "Dental Implants". We limited our results to humans, to articles published in the English language; and, in the time range of 1966 to November 2008. The references of the retrieved articles were also searched.

The inclusion and exclusion criteria

The studies included in this review met the following inclusion criteria: (1) only relevant data on bone augmentation induced by the growth factors; (2) only randomized, non-randomized clinical trials, cohort studies, case-control studies, and case reports; (3) only studies with a clearly written amount and concentration of growth factors or using the kit with fixed concentration of growth factors; (4) only studies with a clearly defined baseline; and (5) only studies with the application of titanium root-form implants. The most recent report was used if more than one publication referred to the same data. The studies that did not meet all the inclusion criteria were excluded from the review. The studies that dealt with the following topics were excluded: (1) *in vitro* animal studies; (2) studies using gene therapy; (3) studies with a focus on periodontal regeneration; (4) studies reporting systemic treatment outcomes; (5) craniofacial surgery for total or partial reconstruction of mandibles/maxillas; (6) cleft lip and palate surgeries; (7) distraction osteogenesis; (8) osseointegration; (9) implant anchor; (10) immediate loading or (11) orthopedic surgeries. Each retrieved citation was reviewed by two independent reviewers (K.S., O.M.). Most of the citations were excluded immediately, due to the information provided by the title or the abstract. If the citation could not be excluded immediately because of its equivocal nature, then the complete article was selected by the two reviewers. Any disagreement between the reviews was resolved by a consensus. To avoid any bias, the search

process was blinded to the names of the authors, to the names of institutions, and to the names of the journals.

The data extraction

The data were independently extracted by two reviewers using data extraction tables. Any disagreements were discussed until they were resolved by a consensus. The following information were extracted: the authors, the year of publication, the study design, the number of patients, the mean age of the patients, the follow-up period, the adverse event, the applied dose of growth factor, the carrier system, the control group, the type and the dimension of the defect, the decrease in the defect of height/increased bone height/width, the newly formed bone, and the new bone density.

Result

The study characteristics

The PubMed search identified a total of 119 citations. However, most of them were excluded immediately due to the information provided by the title or the abstract (Fig. 1). Only 20 articles were selected for further text review [11–30]. The main reasons for excluding some studies ($n = 13$), after the full text was obtained, were as follows: poor-quality data for bone augmentation induced by growth factors, any reports based on animal studies, and a lack of or insufficient discussion of the clinical, radiographic, or histological treatment outcomes (only descriptive presentation of results). Of the seven eligible articles, three studies reported on bone augmentation with rhBMP-2 [14,15,17], three studies discussed the effect of rhPDGF [11–13], and one study examined the effect of Plasma-Rich Growth Factor (PRGF) [16]. Two of the rhBMP-2 studies were randomized control trials (RCT) with a clearly stated random allocation of subjects. The other BMP-2 study was a prospective, human clinical trial without a control. All of three rhPDGF studies and the PRGF study were case reports.

Table 1 shows the characteristics of the included studies. A total of 76 patients were treated with growth factors for local intra-oral bone regeneration. The mean age of the patients was 54.8 years and the mean follow-up period was 47.1 months. Table 2 shows the operative data reported in the included studies. The growth factors were always administered locally, and the root form dental implant was used in every study. The applied dose of the rhBMP-2 ranged from 0.43 to 1.5 mg/ml or from 0.2 to 24 mg/patient. However, the rhPDGF and the PRP studies lacked this type of information. Two different carrier systems were used for the application of rhBMP-2. An absorbable collagen sponge (ACS) was used in two studies [14,17], whereas rhBMP-2 was applied to a demineralized bovine bone matrix (xenogenic bone substitute mineral, Bio-Oss[®]) in another study [15]. With respect to the application of rhPDGF, the carriers used were Bio-Oss[®], beta-tricalcium phosphate (β -TCP) and a freeze-dried mineralized bone allograft (FDBA). For the PRGF treatment, a combination of Bio-Oss[®] and autogenous bone was used. The types of local bone augmentations observed were sinus floor augmentations [14,16,17], preservations of extraction socket [13,17], alveolar ridge bone augmentation [11], and lateral ridge augmentation in combination with

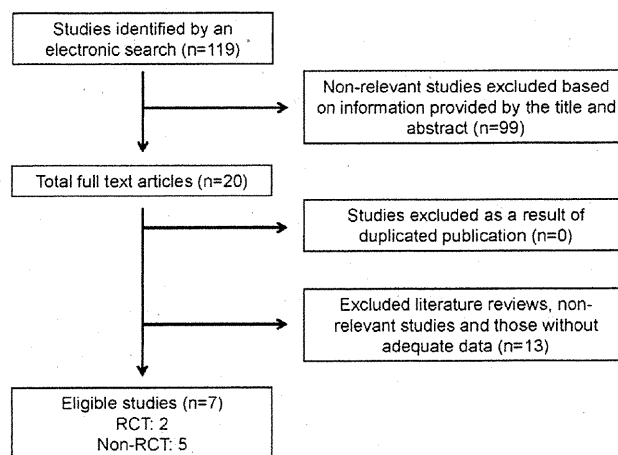


Figure 1 Outline of the literature search.

simultaneous implant placement [12,15,16]. A meta-analysis of the outcomes was not performed because of the heterogeneity of the studies (various indications, RCT, or cohort)

Bone height increase/defect size decrease

An increase in bone height, ranging from 10.16 ± 4.7 to 9.47 ± 5.72 mm for the sinus lift procedures, and a change in bone depth of 6.8 ± 0.2 mm, for the extraction socket augmentations, were reported for the sites treated with rhBMP-2 (Table 3). Two RCTs included control groups without the application of the rhBMP-2 [14,15]. In comparison to the controls, the effect of rhBMP-2 showed substantial variability. Boyne et al. presented negative data for the bone height, and the average gain in the bone height was 11.29 ± 4.12 mm for the control sites and 9.47 ± 5.72 mm for test sites with a low dose of rhBMP-2, respectively. There were no statistically significant differences in the control group with respect to the increase in ridge height, and the decrease in ridge width with the use of rhBMP-2 [14]. Only one RCT reported a positive effect in comparison to the control group, when the factor was applied to the lateral ridge augmentation [15].

On the other hand, rhPDGF seemed to have a positive role in enhancing the healing of soft and hard tissues, even though there was no clear mention and evaluation of bone regeneration. The result of the bone augmentation was clearly presented by the use of pictures and dental X-rays that showed successfully filled bone defects within 5–7 months after the operation [11–13].

New bone formation

Jung et al. and Boyne et al. reported the new bone formation as a percentage of the original defect or as new bone density, respectively (Table 3). The dose of the applied factor seemed to have an impact on the treatment outcome, with a higher local bone regeneration for the higher doses of rhBMP-2. For a lower dose of rhBMP-2, a positive, but not a statistically significant effect was observed on the bone formation, whereas, for a higher dose, a positive and statistically significant effect was reported. Boyne et al. reported a significant difference in new bone density in favor of the bone

Table 1 Characteristics of included studies.

| Study | Year of publication | Type of study | Type of surgical procedure | No. of enrolled patient | | | Mean follow-up (month) | Mean age | | M/F ratio | | Outcome |
|----------------|---------------------|----------------------------|--|--------------------------------|---------------|-------|------------------------|---|----------------------|---------------------------------------|---------------|--|
| | | | | Treatment group | Control group | Total | | Treatment group | Control group | Treatment group | Control group | |
| Simion et al. | 2008 | Case report | Alveolar ridge augmentation | 1 | 0 | 1 | 14 | 36 years | — | 0 | — | X-ray |
| Byun et al. | 2008 | Case report | Socket preservation | 1 | 0 | 1 | ND | 65 years | — | 0 | — | X-ray |
| Fagan et al. | 2008 | Case report | Socket preservation | 1 | 0 | 1 | 3 | 52 years | — | 1 | — | X-ray, histology |
| Boyne et al. | 2005 | RCT | Sinus floor augmentation | Low dose: 18; high dose: 17 | 13 | 48 | 52 | Low dose: 57 years \pm 12; high dose: 52 years \pm 7 | 57 years \pm 11 | Low dose: 0.80; high dose: 0.54 | 0.625 | CT, histology, success and survival rate |
| Jung et al. | 2003 | RCT | Alveolar ridge augmentation | 11 | — | 11 | ND | 53 years \pm 16.9 | — | 0.57 | — | Defect filling rate, histology |
| Anitua | 2001 | Case report | Alveolar ridge augmentation Sinus floor elevation | 2 | 0 | 2 | 36 | 61 years \pm 4.2 | — | 1 | — | Histology |
| Cochran et al. | 2000 | Prospective clinical trial | Alveolar ridge augmentation Socket preservation | 12 | 0 | 12 | 36 | ND | — | ND | — | Defect filling rate, histology |

Table 2 Operative data investigated in the included studies.

| Study | Treatment group | | | | Control group Type of bone graft | Implant system | Number of implant |
|----------------|--|--|---|---|-------------------------------------|---|-------------------|
| | Type of growth factor | Dose of growth factor | Delivery vehicle | Concentration of growth factor | | | |
| Simion et al. | rhPDGF-BB (GEM21S [™] ; BioMimetic) | ND | Bio-Oss [™] + autogenous bone | 1.2 mg/ml | — | MK3 Natural Platform 3.3 mm × 15 mm, Speedy Groovy 4 mm × 15 mm, Nobel biocare | 2 |
| Byun et al. | rhPDGF-BB (GEM21S [™] ; BioMimetic) | ND | β-TCPalloplast, autogenous bone | 0.3 mg/ml | — | Tapered ScrewVent 3.7 mm × ND mm, Zimmer Dental | 1 |
| Fagan et al. | rhPDGF-BB (GEM21S [™] ; BioMimetic) | ND | FDBA | 0.3 mg/ml | — | Osseotite implant 4 mm × 13 mm, BIOMET/3i | 1 |
| Boyne et al. | rhBMP-2 (Medtronic) | Low dose: 8.9 mg (5.2–12.0 mg); high dose: 20.8 mg (10.8–24.0 mg) | Autogenous bone or ACS | Low dose: 0.75 mg/ml; high dose: 1.5 mg/ml | Autogenous bone graft | ND | 219 |
| Jung et al. | rhBMP-2 | 0.18 mg | Bio-Oss [™] | 0.5 mg/ml | Bio-Oss [™] | Machine surface, Nobel biocare | 34 |
| Anitua | PRGF (PRP) | ND | Bio-Oss [™] + autogenous bone | ND | — | ND | 5 |
| Cochran et al. | rhBMP-2 | Alveolar ridge augmentation 0.27 mg (0.1–0.9 mg), Socket preservation 0.83 mg (0.2–1.7 mg) | ACS | 0.43 mg/ml | — | Titanium plasma sprayed implant | 13 |